ILASS 2008
Sep. 8-10, 2008, Como Lake, Italy

Paper ID ILASS08-13-7

SPREADING AND RECEDING PROCESSES OF IMPACTING LIQUID DROPS ON GROOVED SURFACES

R. Kannan*, D. Sivakumar°

*Research Student, Department of Aerospace Engineering, Indian Institute of Science, Bangalore 560012, India
°Assistant Professor, Department of Aerospace Engineering, Indian Institute of Science, Bangalore 560012, India

Abstract

The impact of inertia dominated water drops with Weber number in the range 48 -167 on grooved target surfaces is studied experimentally. The target surfaces were comprised of surface structures of unidirectional grooves. The groove depth was varied significantly between the grooved target surfaces. The spreading and receding process of impacting liquid drops were visualized both along the groove direction and perpendicular to the groove direction. The geometry of groove structure influences the drop impact process in two ways: 1) it modifies the wettability characteristics of target surfaces; 2) it provides a larger volume fraction of droplet liquid to spread along the groove direction. The former influences the receding and rebounding characteristics of impacting liquid drops whereas the later develops anisotropy in the droplet spreading. The results reveal that the grooved surface with larger groove depth yields higher liquid contact angle, which in turn develops stronger receding and rebounding characteristics for the impacting drops. In addition the present analysis shows that the anisotropy in droplet spreading is strongly influenced by the groove depth.

Introduction

The impact of inertia dominated liquid drops on a solid target surface has been extensively analyzed in the literature.[1,2] The phenomenon is encountered in several practical applications such as inkjet printing, spray coating process, pesticide spraying, etc. Surface topography of the target surface is one of the major parameters which influences the outcomes of drop impact process. This occurs via a modification of surface wettability characteristics.[3,4] Wenzel's equation[3] and Cassie-Baxter relationship[4] determine the equilibrium liquid contact angle on a rough surface. The Wenzel's model[3] assumes that the droplet liquid wets and fills pores and grooves present on the rough surface completely whereas the model by Cassie and Baxter[4] considers an interface composed of both solid and ambient gas under the liquid drop. The effect of surface topography on the impact of inertia dominated drops has been studied in the literature by varying surface roughness of target surfaces.[5-11] These studies suggest that roughening a target surface by increasing the mean surface roughness, R_a promotes the splashing of impacting drops. The random crest and trough patterns of a rough surface may be introducing perturbations to the lamella front formed immediately after the start of impact, and these perturbations grow with time and lead to enhanced droplet splashing.[10]

Recently there is an enormous interest towards the understanding of the effect of surface topography on droplet spreading in the context of development of superhydrophobic surfaces.[12-15] A systematic arrangement of pillar like structures on a surface of hydrophobic material increases droplet contact angles as high as 170 degrees with low contact angle hysteresis.[12-17] On a superhydrophobic surface a water droplet takes the configuration considered by Cassie and Baxter.[4] A strong correlation between the surface features of syperhydrophobic surfaces and the surface wetting characteristics exists as per these studies. Bartolo et al.[18] and Reyssat et al.[19] studied the impact of liquid drops on superhydrophobic surfaces using high speed imaging systems. Liquid droplets impinging on these superhydrophobic surfaces bounce-off for a certain range of impact velocity and liquid impales into the surface structure for higher impact velocities. Sivakumar et al.[20] studied the impact of high inertia drops on model rough surfaces comprising of square-top asperities and reported that surface texture pattern governs the spreading pattern of impacting drops. A recent investigation of drop impacts on surfaces with similar textured pattern by Xu[21] showed that the splash occurs predominantly along the diagonal directions of the textured surfaces.

A rough target surface has an irregular surface topography comprising grooves and asperities of different sizes. Random distribution of surface grooves and asperties poses difficulties to understand the effect of surface topography on the impact of liquid drops. Model rough surfaces exhibiting a regular surface profile have often been used to describe the effect of surface roughness on surface wettability behavior.[16,17] This paper deals with the impact of inertia dominated liquid drops on model surfaces comprising unidirectional groove structure. Experimental and numerical studies have been reported in the literature on the spreading of droplet liquid on model rough surfaces comprising of unidirectional grooves.[22-28] A target surface comprising parallel grooves develops different wetting characteristics in directions along the grooves and perpendicular to the grooves.[26-28] The apparent contact angle made by droplet liquid in the groove direction is smaller than that measured perpendicular to the groove direction. In this paper experimental results on the impact of inertia dominated liquid drops on grooved surfaces (two surfaces) are presented.

Groove structure for the grooved surfaces were selected in such a way that the surfaces exhibit different wettability characteristics. Although the spreading of droplet liquid on grooved surfaces was investigated earlier,[22-28] the results on the quantitative description of both the spreading and receding processes of impacting liquid drops, particularly for inertia dominated drops, are very limited in current literature.

Experimental details

Experiments of drop impacts were carried out using an experimental apparatus sketched in Fig. 1 and its salient details are described in Sivakumar et al.[20] The apparatus captures a single image of an impacting drop during a drop impact experiment at a desired time interval from the start of impact. Temporal image sequences of the impacting drop were constructed from the images captured at varying time lapse from the start of impact by conducting several identical drop impact experiments. This procedure was followed in several earlier studies.[29-31] Liquid drops were generated by using a flat tipped hypodermic needle of internal and external diameters 0.25 mm and 0.37 mm respectively. Additional details of drop

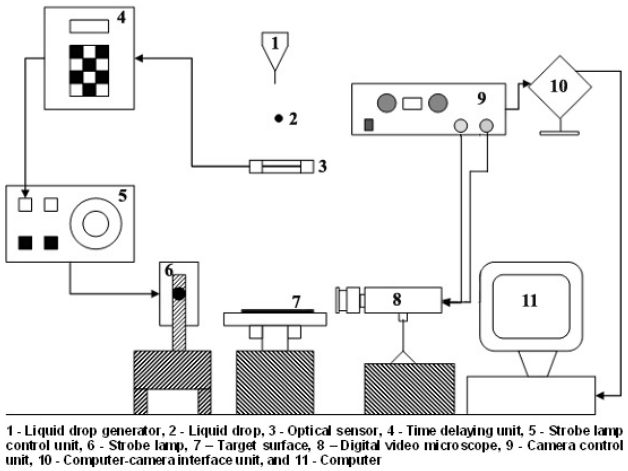

1 - Liquid drop generator, 2 - Liquid drop, 3 - Optical sensor, 4 - Time delaying unit, 5 - Strobe lamp control unit, 6 - Strobe lamp, 7 – Target surface, 8 – Digital video microscope, 9 - Camera control unit, 10 - Computer-camera interface unit, and 11 - Computer

Fig. 1 A schematic of the experimental apparatus.

mm. Major geometrical dimensions of the grooved surfaces, groove width, b, groove depth, d and width of solid pillar separating any two successive grooves, w are given in Table I. The grooved surface *TS1* was prepared using photolithography techniques. Figure 2 shows a scanning electron microscopy (SEM) image of the grooved surface *TS1* along with a surface profile plot obtained using 2D stylus surface profile meter. The grooved surface *TS2* was prepared via laser based machining process and a high resolution video image of its sectional view is given in Fig. 3. Surface roughness for the tops of surface pillars of the grooved surfaces was identical to

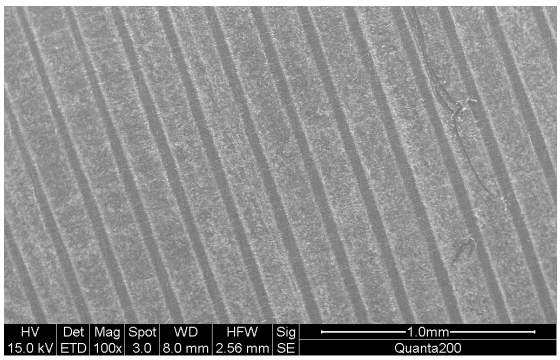

(a)

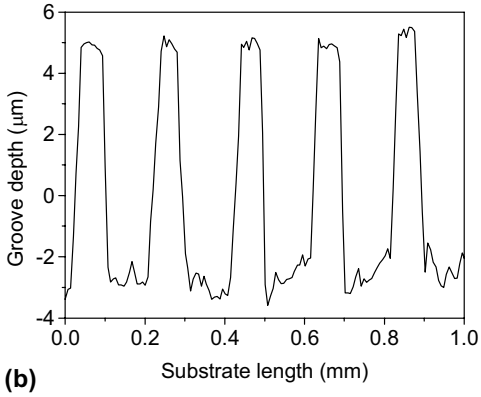

(b)

Fig. 2 SEM image and surface profile plot for the grooved surface *TS1*. Lighter region in the SEM image corresponds to the grooves.

Table I Geometric parameters of the grooved surfaces

Surfaces	d (μm)	b (μm)	w (μm)
TS1	7.5	136	66
TS2	220	173	126

production including the repeatability associated with the drop production process are given in Kannan and Sivakumar.[32] Distilled water with density, $\rho = 996$ kg/m^3, surface tension, $\sigma = 0.073$ N/m and viscosity, $\mu = 0.89\times10^{-3}$ kg/ms was used as the droplet liquid. Diameter of an impacting drop, D_o was measured from its image captured just prior to the impact. Velocity of an impacting drop, U_o was estimated from the distance between the needle tip and the target surface, H, and different values of U_o were simulated by varying H.

The target surfaces, two grooved surfaces (*TS1* and *TS2*) and one smooth surface (*RS1*), made of stainless steel were used in the study. The smooth surface was prepared using a diamond paste polishing machine and the value of R_a was measured from surface profile plot as 0.013 μm. The grooves were unidirectional for the grooved surfaces and were formed on finely polished steel surfaces of size 20 mm x 20

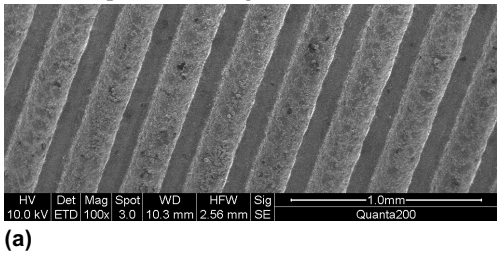

(a)

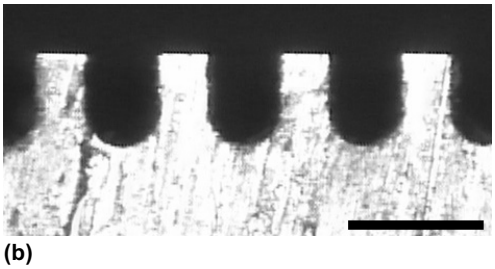

(b)

Fig. 3 SEM image and front view of the grooved surface *TS2*. Lighter region in the SEM image corresponds to the grooves.

that of the smooth surface. However additional surface roughness was introduced on the bottom surfaces of the grooves by the fabrication process. An examination of the bottom surfaces of the grooves for *TS1* and *TS2* with the help of optical profilometer gave the values of R_a in the ranges 0.2 – 0.37 μm and 1.09 – 1.47 μm respectively. The grooved surface *TS1* was different from *TS2* mainly from the fact that the value of *d* for *TS2* was substantially larger (around 29 times) than that of *TS1*. The other geometrical parameters of the grooved surface *b* and *w* were comparable in order of magnitude between *TS1* and *TS2*.

An impacting drop was characterized in terms of Weber number, *We* which was calculated using the expression $\mathrm{We} = \rho U_o^2 D_o/\sigma$, where ρ is the density of droplet liquid and σ, the surface tension. The images of spreading drops were obtained to illustrate both droplet spreading on the grooved surface along the groove direction and droplet spreading on the grooved surface perpendicular to the groove direction. The images were recorded with 768 × 576 pixel resolution to a computer. The temporal measurements of spreading drop diameter, *D* on the surface top and drop height at the center, *Z* from the surface top were obtained from the images captured as function of time. The measurements of *D* and *Z* were nondimensionalized with D_o and the time lapse, *t* measured from the instant at which the impacting drop touches the top of the target surface was nondimensionalized as $\tau = tU_o/D_o$.

Wettability characteristics of the grooved surfaces

Table II Measurements of θ_e for the target surfaces

Surfaces	$\theta_{e,//}$ (deg)*	$\theta_{e,\perp}$ (deg)**
TS1	68	77
TS2	106	135
RS1	80	80

#Viewed along the groove direction
##Viewed perpendicular to the groove direction

Attem pts were made to elucidate the wettability behavior of the grooved surfaces studied here. A liquid volume of 8 *μL* was gently placed on the target surfaces using a micro pipette in these experiments. Images of droplet shapes were captured within 15 seconds from the instant of placement of liquid volume. For the grooved surfaces, the images were captured to visualize the position of liquid front both along the groove direction and perpendicular to the groove direction. Figure 4 shows images of droplet shapes attained by the liquid volume on the grooved surfaces *TS1* and *TS2*. The figure also illustrates the shape of droplet observed on the smooth surface, *RS1*. As seen in Fig. 4(a) no significant changes in the

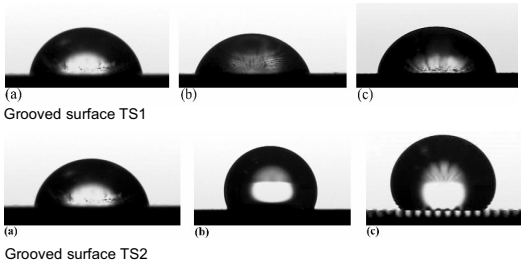

Fig. 4 Wettability characteristics of the target surfaces. (a) Smooth surface, (b) Grooved surface – view is along the groove direction, and (c) Grooved surface – view is perpendicular to the groove direction.

shape of droplet resting on the grooved surface *TS1*. It is clear from the images given in Fig. 4(b) that the droplet on the grooved surface *TS2* is partially supported by the ambient air. In other words the droplet takes the configuration considered by Cassie and Baxter.[4] These images were used to extract the measurement of liquid contact angle, θ_e on the target surfaces and the values are given in Table II. For each case, the listed value of θ_e was taken as the mean value from 10 independent experiments.

The values of θ_e obtained for the grooved surface *TS1* show that the presence of groove structure makes *TS1* more hydrophilic. This is in line with Wenzel's equation, $\cos\theta_e^r = r\cos\theta_e^s$, which shows that the liquid contact angle on a rough surface (θ_e^r) is lesser than the liquid contact angle on the corresponding flat surface (θ_e^s) if $\theta_e^s < 90$ deg. A large groove aspect ratio (*b/d*) of the grooved surface *TS1* makes the droplet liquid to follow the surface structure. The measurements of θ_e given in Table II for the grooved surface *TS2* indicate that the presence of groove structure makes *TS2* as hydrophobic surface. This is attributed to the substantial increase in groove depth of *TS2* compared to *TS1*. Thus the grooved surface *TS1* and *TS2* exhibit completely different wettability characteristics caused by the variation in groove depth.

Results and discussion

Figure 5 illustrates the image sequences of spreading

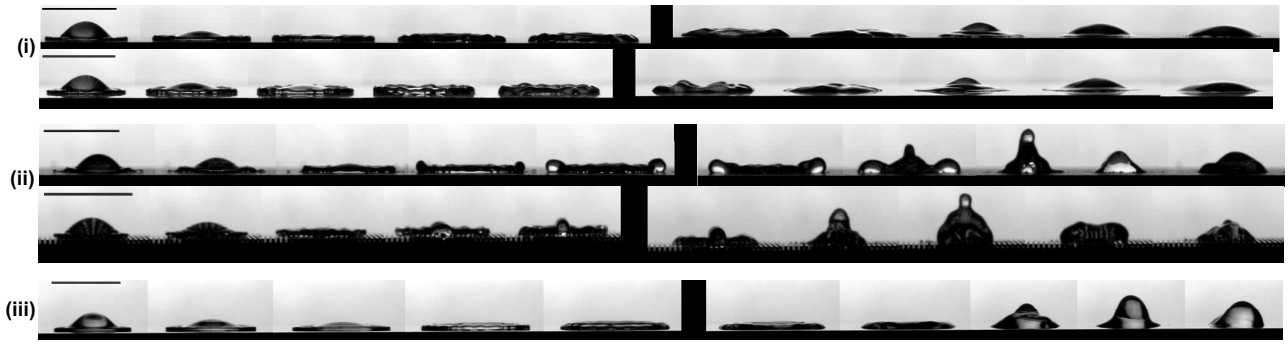

Fig. 5 Image sequences illustrating the spreading and receding processes of impacting liquid drops with *We* ≈ 82 on the grooved surfaces. (i) Grooved surface *TS1*, (ii) Grooved surface *TS2*, and (iii) Smooth surface *RS1*. For the grooved surfaces, the groove direction is from left to right of the page for the first image sequence and is perpendicular to the surface of the page for the second image sequence. Value of τ for the images is increasing from left to right. The line shown in the image sequences corresponds to a scale length of 5 mm.

and receding processes of impacting liquid drops with *We* ≈ 82 on the grooved surfaces *TS1* and *TS2*. The corresponding image sequences obtained for similar *We* on the smooth surface, *RS1* are also given in Fig. 5 for comparison purposes.

- The receding and rebounding of droplet liquid on the grooved surface *TS1* are lesser intense than that seen on the smooth surface whereas those observed on the grooved surface *TS2* are more intense.

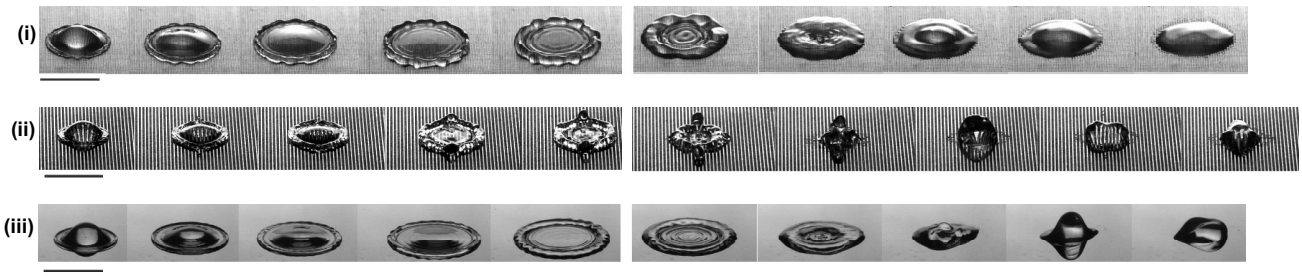

Fig. 6 Image sequences illustrating the spreading and receding processes of impacting liquid drops with *We* ≈ 82 on the grooved surfaces. (i) Grooved surface *TS1*, (ii) Grooved surface *TS2*, and (iii) Smooth surface *RS1*. For the grooved surfaces, the groove direction is from the top to bottom. Value of τ for the images is increasing from left to right. The line shown in the image sequences corresponds to a scale length of 5 mm.

During the impact process, the impacting drop spreads out radially from the impact point, reaches a maximum diameter, D_{max} and thereafter recedes towards the impact point. Similar image sequences of drop impact process were constructed 1from the images captured by viewing the impacting drops from the top. Typical of such image sequences are shown in Fig. 6 for the drop impact condition as in Fig. 5. A comparison of image seuqences between the grooved surfaces and the smooth surface reveals the following.

- The spreading front of impacting drops on the grooved surfaces exhibits features which are different from those seen with the smooth surface. A larger rim in the periphery of spreading drops is seen during the impact process on the grooved surfaces. In general the liquid lamella seen on the grooved surfaces is more perturbed than that seen on the smooth surface.
- The receding process of impacting drops on the grooved surfaces is altered severely compared to that seen on the smooth surface.

The quantitative variation of D with τ obtained during the spreading and receding process of impacting liquid drops of different *We* with the grooved surfaces is shown in Figs. 7 and 8. The plots also include the measurements of D obtained with the smooth surface for similar impact conditions. Figure 7 shows the trends of variation of $D_{//}$ with τ for the grooved surfaces. Note that droplet spreading along the groove direction is almost identical to the spreading on a smooth surface and one can expect that the variation of $D_{//}$ versus τ for the grooved surfaces follows the trend observed with the smooth surface. It is observed from Fig. 7 that the droplet spreading on the grooved surface follows the variation of D with τ obtained for the smooth surface during the early part of drop impact process only. As the droplet spreading process is purely driven by the kinetic energy of impacting drop during low τ values, the influence of surface structure on the droplet spreading process is almost negligible as seen in Fig. 7. However the influence of surface structure is observed during

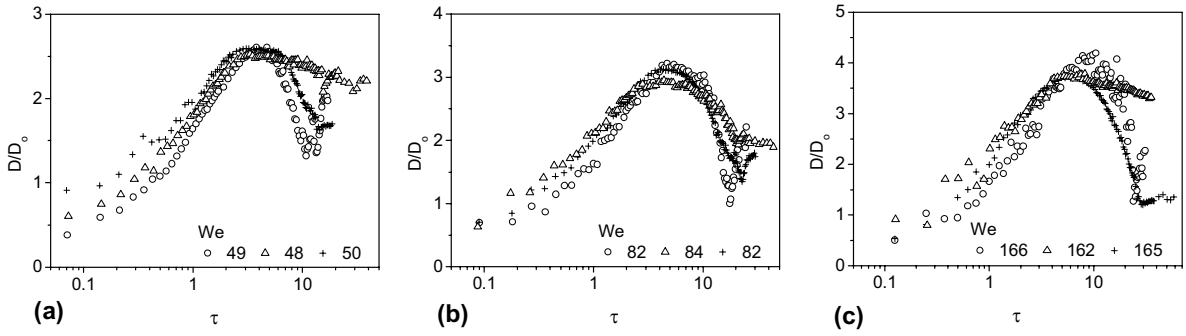

Fig. 7 Normalized spreading drop diameter measured along the groove direction ($D_{//}$ / D_o) with time during the spreading and receding process for the impact of liquid drops with different *We* on the grooved surfaces.
+ Smooth surface, Δ Grooved surface *TS1*, and ○ Grooved surface *TS2*.

- The groove direction influences the spreading and receding process of impacting drops. This can be clearly seen by comaring the image sequences of drop impact process along the groove direction and perpendicular to the groove direction given in Figs. 5 and 6. This effect is mimimal for the grooved surface *TS1* compared to the grooved surface *TS2*.

the receding of droplet liquid. This can be seen from the image sequences given in Fig. 5. For instance the rebounding liquid volume on the grooved surface *TS1* is significantly smaller compared to that seen on the smooth surface. Data analysis reveals that that the grooved surface *TS1* limits the receding of droplet liquid along the groove direction at low *We* as seen in Fig. 7(a). In moderate *We*, the variation of $D_{//}$ versus τ in the receding process for the grooved surface *TS1* almost follows

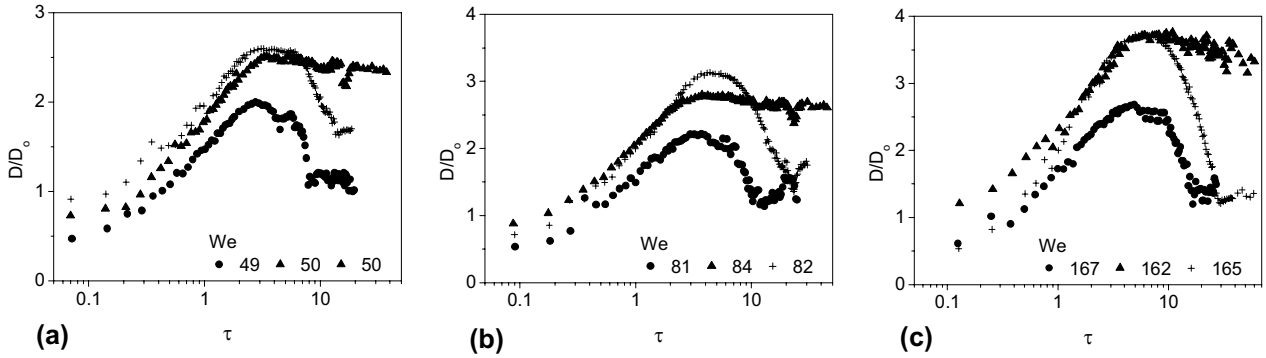

Fig. 8 Normalized spreading drop diameter measured perpendicular to the groove direction ($D_{\perp}$) with time during the spreading and receding process for the impact of liquid drops with different *We* on the grooved surfaces.
+ Smooth surface, ▲ Grooved surface *TS1*, and ● Grooved surface*TS2*.

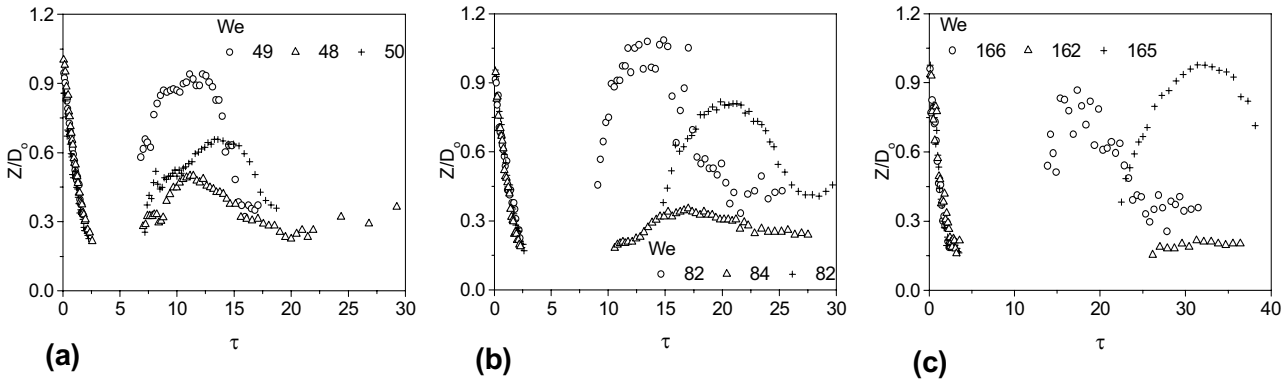

Fig. 9 Normalized droplet height measured at the droplet center with time during the impact of liquid drops with different *We* on the grooved surfaces. + Smooth surface, Δ Grooved surface *TS1*, and ○ Grooved surface*TS2*.

that observed with the smooth surface as seen in Fig. 7(b). Based on a similar analysis, it is observed that the receding of droplet liquid on the grooved surface *TS2* follows the trend observed with the smooth surface for the drop impact conditions studied here. It is also observed from Figs. 7(a) and 7(b) that the grooved surface *TS2* intensifies the receding of droplet liquid (the sharp decrease of $D_{//}$ after reaching a maximum droplet diameter during the spreading process as indicated by open circles in Figs. 7(a) and (b)).

Figure 8 shows the varation of droplet spreading diameter perpendicular to the groove direction ($D_{\perp}$) for the grooved surfaces. The grooves restrict the receding of droplet liquid perpendicular to the grooved direction on the grooved surface *TS1* for all *We* conditons. However, a well defined receding process is observed on the grooved surface TS2 as seen in Fig. 8. A more striking feature in Fig. 8 is that $D_{\perp}$ measured on the grooved surface *TS2* is significantly lesser than that measured on the grooved surface *TS1* and the smooth surface. The presence solid pillars restricts the movement of droplet liquid perpendicular to the groove direction. From the measurements given in Figs. 7 and 8, it is clear that the groove structure of *TS2* develops a larger level of anisotropy in the droplet spreading process. Figure 9 shows the instantaneous variation of Z/D_o obtained during the impact of liquid drops on the grooved surfaces for different *We*. The plots given in Fig. 9 clearly support a stronger rebounding behavior of the impacting drops on the grooved surface *TS2*. The groove structure of *TS1* dramatically suppresses the rebounding of droplet liquid as seen in Figs. 9(b) and 9(c).

The experimental results shown in the previous section clearly demonstrates that the presence of groove structure on the target surface influences the impact process of liquid drops. In line with previous works of wettability behavior of surfaces with different surface topography, the presence of groove structure modifies the wettability characteristics of the grooved surfaces. A groove structure comprising smaller depth grooves on the smooth surfaces makes the surface more hydrophilic as in the case of the grooved surface *TS1*. The increase in hydrophilicity may be responsible for the less intensive receding and rebounding process observed on the grooved surface *TS1*. In a similar manner a groove structure comprising larger depth grooves on the smooth surface makes the surface more hydrophobic as in the case of the grooved surface *TS2*. The effect of enhanced hydrophobicity of the grooved surface *TS2* can be seen from a stronger rebounding of droplet liquid observed during the impact of liquid drops. It must be mentioned here that the grooved surfaces *TS1* and *TS2* differ mainly on the groove depth. Recently Barbieri et al.[33] studied wetting transition between the Cassie-Baxter[4] and Wenzel[3] regimes of water drops on different superhydrophobic surfaces comprising flat-top pillars. For a given surface structure, it was found that an increase in pillar height makes water drops to enter the Cassie-Boxter regime from the Wenzel regime. A similar effect is observed here between the grooved surfaces *TS1* and *TS2*.

A comparison measurements given in Figs. 7 and 8 show that the dynamics of droplet liquid is more intense along the grooved direction. This may be understood from that fact that the groove direcion offers no resistance to the spreading/receding drop whereas the droplet liquid

experiences resistance in the direction perpendicular to the grooves due to the presence of solid pillars. The droplet liquid, on its way along the groove direction, encounteres edges of pillars which dissipates energy. This may be the reason for a complete arrest in the movement of droplet liquid during the receding process on the grooved surface TS1. A significant decrease in $D_{max,\perp}$ for the grooved *TS2* as seen in Fig. 8 may be attributed to the larger groove depth which makes a larger fraction of droplet liquid to flow along the groove direction.

Conclusions

This experimental study on the impact of inertia dominated liquid drops on grooved target surfaces documents the influence of groove structure geometry on the spreading and receding processes of droplet liquid. The groove structure alters the wettability characteristics of grooved surfaces, which in turn changes the receding and rebounding characteristics of impacting liquid drops. It is observed that the groove structure geometry restricts the dynamics of droplet liquid in the direction perpendicular to the groove direction which results in spreading anisotropy. A groove structure which adsorbs a larger fraction of droplet liquid is prone to develop more spreading anisotropy of droplet liquid on grooved surfaces.

References

[1]M. Rein, "Phenomena of liquid drop impact on solid and liquid surfaces," Fluid Dyn. Res. **12**, 61 (1993).

[2]A. L. Yarin, "Drop impact dynamics: Splashing, spreading, receding, bouncing….," Ann. Rev. Fluid Mech. **38**, 159 (2006).

[3]R. N. Wenzel, "Resistance of solid surfaces to wetting by water," Ind. Eng. Chem. **28**, 988 (1936).

[4]A. B. D. Cassie and S. Baxter, "Wettability of porous surfaces," Trans. Faraday Soc. **40**, 546 (1944).

[5]O. G. Engel, "Water drop collisons with solid surfaces," J. Res. Natl. Bur. Stand. **54**, 281 (1955).

[6]Z. Levin and P. V. Hobbs, "Splashing of water drops on solid and wetted surfaces: Hydrodynamics and charge separation," Philos. Trans. R. Soc. London Ser. A **269**, 555 (1971).

[7]C. D. Stow and M. G. Hadfield, "An experimental investigation of fluid flow resulting from the impact of a water drop with an unyielding dry surface," Proc. R. Soc. London Ser. A **373**, 419 (1981).

[8]C. Mundo, M. Sommerfeld, and C. Tropea, "Droplet-wall collisions: Experimental studies of the deformation and breakup process," Int. J. Multiphase Flow **21**, 151 (1995).

[9]K. Range and F. Feuillebois, "Influence of surface roughness on liquid droplet impact," J. Colloid Interface Sci. **203**, 16 (1998).

[10]M. Bussmann, S. Chandra, and J. Mostaghimi, "Modeling the splash of a droplet impacting a solid surface," Phys. Fluids **12**, 3121 (2000).

[11]L. Xu, "Liquid drop slpashing on smooth, rough, and textured surfaces," Phys. Rev. E **75**, 056316 (2007).

[12]S. Shibuichi, T. Onda, N. Satoh, and K. Tsujii, "Super water-repellent surfaces resulting from fractal structure," J. Phys. Chem. **100**, 19512 (1996).

[13]D. Oner and T. J. McCarthy, "Ultrahydrophobic surfaces: Effects of topography length scales on wettability," Langmuir **16**, 7777 (2000).

[14]D. Richard and D. Quéré, "Bouncing water drops," Euro. Phys. Lett. **50**, 769 (2000).

[15]J. Bico, U. Thiele, and D. Quéré, "Wetting of textured surfaces," Colloids and Surfaces A **206**, 41 (2001).

[16]S. J. Hitchcock, N. T. Carroll, and M. G. Nicholas, "Some effects of substrate roughness on wettability," J. Mat. Sci. **16**, 714 (1981).

[17]H. Nakae, R. Inui, Y. Hirata, and H. Saito, "Effects of surface roughness on wettability," Acta Mater. **46**, 2313 (1998).

[18]D. Bartolo, F. Bouramrirene, É. Verneuil, A. Buguin, P. Silberzan, and S. Moulinet, "Bouncing or sticky droplets: Impalement transitions on syperhydrophobic micropatterned surfaces," Europhys. Lett. **74**, 299 (2006).

[19]M. Reyssat, A. Pépin, F. Marty, Y. Chen, and D. Quéré, "Bouncing transitions on microtextured materials," Europhy. Lett. **74**, 306 (2006).

[20]D. Sivakumar, K. Katagiri, T. Sato, H. Nishiyama, "Spreading behavior of an impacting drop on a structured rough surface," Phys. Fluids **17**, 100608 (2005).

[21]L. Xu, "Liquid drop splashing on smooth, rough, and textured surfaces," Phys. Rev. E **75**, 056316 (2007).

[22]J. F. Oliver, C. Huh, and S. G. Mason, "The apparent contact angle of liquids on finely-grooved solid surfaces – A SEM study," J. Adhesion **8**, 223 (1976).

[23]J. F. Oliver, C. Huh, and S. G. Mason, "An experimental study of some effects of solid surface roughness on wetting," Colloids and Surfaces **1**, 79 (1980).

[24]R. G. Cox, "The spreading of a liquid on a rough solid surface," J. Fluid Mech. **131**, 1 (1983).

[25]S. Gerdes and G. Ström, "Spreading of oil droplets on silicon oxide surfaces with parallel v-shaped channels," Colloids and Surfaces A **116**, 135 (1996).

[26]J. Bico, C. Tordeux, and D. Quéré, "Rough wetting," Europhys. Lett. **55**, 214 (2001).

[27]Y. Chen, B. He, J. Lee, and N. A. Patankar, "Anisotropy in the wetting of rough surfaces," J. Colloid Interface Sci. **281**, 458 (2005).

[28]Y. Zhao, Q. Lu, M. Li, and X. Li, "Anisotropic wetting characteristics on submicrometer-scale periodic grooved surface," Langmuir **23**, 6212 (2007).

[29]R. Rioboo, M. Marengo, and C. Tropea, "Time evolution of liquid drop impact onto solid, dry surfaces," Exp. Fluids **33**, 112 (2002).

[30]S. Shakeri and S. Chandra, "Splashing of molten tin droplets on a rough steel surface," Int. J. Heat Mass Transf. **45**, 4561 (2002).

[31]S. Šikalo, M. Marengo, C. Tropea, and G. N. Ganic, "Analysis of impact of droplets on horizontal surfaces," Exp. Thermal Fluid Sci. **25**, 503 (2002).

[32]R. Kannan and D. Sivakumar, "Impact of liquid drops on a rough surface comprising microgrooves," Exp. Fluids **44**, 927 (2008).

[33]L. Barbieri, E. Wagner, P. Hoffmann, "Water wetting transition parameters of perfluorinated substrates with periodically distributed flat-top microscale obstacles," Langmuir **23**, 1723 (2007).